Defence Science Journal, Vol. 72, No. 1, January 2022, pp. 30-39, DOI : 10.14429/dsj.72.16542
© 2022, DESIDOC

# Heat Transfer Modelling and Simulation of a 120 mm Smoothbore Gun Barrel During Interior Ballistics

Çiğdem Susantez[*] and Aldélio Bueno Caldeira[#]

[*]Trakya University, Engineering Faculty, Mechanical Engineering Department, Edirne - 22030, Turkey
[#] Management and Technological Innovation Agency, Brazilian Army, Rio de Janeiro - 23020-470, Brazil
[*]E-mail: cigdemsusantez@trakya.edu.tr

**ABSTRACT**

Understanding the heat transfer phenomenon during interior ballistics and consequently presenting a realistic model is very important to predict the temperature distribution inside the cannon barrel, which influences the gun wear and the cook-off. The objective of this work is to present a new detailed numerical model for the prediction of thermal behaviour of a cannon barrel by combining PRODAS interior ballistics simulation with COMSOL simulation. In this study, a numerical model has been proposed for the heating behaviour of a 120 mm smoothbore cannon barrel, taking into account the combustion equation of the JA-2 propellant. Temperature dependent thermophysical properties of product gases were used for the calculation of the convective heat transfer coefficient inside the barrel. Projectile position, velocity of the projectile, gas temperature inside the barrel, volume behind the projectile and mass fraction during interior ballistics have been obtained by PRODAS software and used in the numerical model performed by COMSOL multiphysics finite element modelling and simulation software. Temperature simulations show that maximum wall temperature inside the cannon barrel is observed after 3 ms from fire, when maximum value of the convective heat transfer coefficient inside the barrel is observed. The results reveal that the convective heat transfer coefficient of burned gases inside the gun has major effect than the burned gas temperature on the heat transfer phenomenon.

**Keywords:** Interior ballistics; Cannon barrel; Finite element method; Transient heat transfer

## NOMENCLATURE

| | |
|---|---|
| *a, b, c, d, e, f* | Mole numbers of combustion product of $C_aH_bN_cO_dCl_eS_f$ |
| $a_1$, $b_1$, $c_1$, $d_1$, $e_1$, $f_1$ | Mole numbers of ingredients of JA-2 |
| $c_{steel}$ | Specific heat of steel |
| $D$ | Diameter |
| $h_{in}$ | Internal convection heat transfer coefficient before the projectile |
| $h_s$ | Convection heat transfer coefficient inside the barrel, function of $h_{in}$ and $S$, Eqn (9) |
| $h_{out}$ | Convection heat transfer coefficient outside the barrel |
| $k$ | Thermal conductivity |
| $L$ | Barrel length |
| $m$ | Mass |
| $Nu$ | Nusselt number |
| $n$ | Proportionality constant |
| $P$ | Breech pressure |
| $Pr$ | Prandtl number |
| $R_{in}$ | Inner radius of the barrel |
| $R_{out}$ | Outer radius of the barrel |
| $R^2$ | Coefficient of determination |
| $Re_{in}$ | Reynolds number inside the barrel |
| $r$, $z$ | Radial and axial coordinates, respectively |
| $S$ | Projectile position |
| $T$ | Temperature |
| $T_0$ | Initial temperature |
| $T_{air}$ | Temperature of the air |
| $T_{ave\_in}$ | Average temperature at the inner surface of the barrel |
| $T_{gas}$ | Temperature of the combustion gases |
| $T_{in}$ | Temperature at the inner surface of the barrel |
| $T_S$ | Temperature of the inside medium of the barrel, function of $T_{gas}$, $T_0$ and $S$, Eqn (8) |
| $T_{max}$ | Highest value of the inside barrel temperature |
| $T_{out}$ | Temperature at the outer surface of the barrel |
| $t$ | Time |
| $V$ | Volume |
| $V_p$ | Velocity of the projectile |
| $V_{wind}$ | Wind velocity |
| $z$ | Distance from breech |
| $\varepsilon$ | Emmisivity of the barrel surface |
| $\mu$ | Dynamic viscosity |
| $\rho$ | Density |
| $\sigma$ | Stefan-Boltzmann constant |

Received : 16 December 2020, Revised : 18 September 2021
Accepted : 23 September 2021, Online published : 05 January 2022

## 1. INTRODUCTION

Interior ballistics is the field of science devoted to research the interaction of the gun, propellant train and projectile, after the fire and while the projectile is inside the gun[1]. This rich branch of the science deals with different phenomena as projectile and barrel dynamics[2], projectile-barrel interaction[3], vibration[4,5], combustion[1], thermodynamics[6], heat transfer[7] among others. Nevertheless, heat transfer is a special process in interior ballistics, since it is related with the large amount of energy released by propellant combustion and with the large amount of energy lost. Consequently, heat transfer influences directly the efficiency of the gun.

After fire, chemical energy of the propellant is converted to kinetic energy of the projectile and also heat due to combustion and friction. Barrel where the combustion takes place is the most important part the gun for the gun life. Heating behaviour of the barrel during interior ballistics is relevant to wear problems, thermomechanical behaviour of the material and also barrel life[7].

As a result, understanding the heat transfer phenomenon during interior ballistics and presenting a numerical model for the heating behaviour of the barrel is a very important subject. Franco and Peter[8] stated the heat transfer coefficient inside the barrel as a function of projectile velocity, mean pressure and gas temperature using Reynold's analogy in their numerical and experimental study. They also showed that steel surface temperature decreases 150K when silicon dioxide coating used on the inner surface of the barrel. Wildegger- Gaissmaier[9] numerically investigated the effects of the wall thickness of the barrel and rate of fire on the barrel temperature. In this study, it is not only showed that barrel temperature increases with the increase of the rate of fire and decrease with the wall thickness, but also it is presented the result that chrome coating on the inner surface of the barrel causes the barrel temperature to increase due to high thermal diffusivity of the chrome. Chen[10], *et al.* used the measured outside temperature of the barrel to numerically estimate inner heat flux and also inner temperature of the barrel. Mishra[11], *et al.* concluded the result that the assumption of constant thermophysical properties causes 3.27% error for the maximum bore surface temperature of the barrel in their numerical study. Şentürk[12], *et al.* investigated the interior ballistics of the 7.62 mm barrel with thermo-mechanical approach by numerical, analytical and experimental methods. They presented temperature and stress distributions on the barrel. Işık and Göktaş[13] inversely found inner heat flux by the measured temperature values on the combustion chamber. They also investigated the effects of time interval between two magazines, number of cartridges in magazines, thicknesses of combustion chamber and cartridge case on cook-off time. Copley and Thomas[14] analytically solved the heat equation for a hollow cylinder subjected to time dependent heat flux on its inner surface. They applied model to barrel heating problem and presented the exponentially decreasing heat flux for the inside boundary condition of the barrel. Hansen and Heiney[15] performed an analytical and experimental study on the projectile motion. They postulated that acceleration of the gases behind the projectile is the main reason of the pressure and density gradients inside the barrel. Bundy[16], *et al.* obtained the temperature values on the 120mm cannon barrel experimentally and also numerically by heat transfer code which is in conjunction with interior ballistic code. Hameed[17], *et al.* found that the cook-off temperature interval of the Bulls Eye propellant is 151.4°C-153.4°C in their experimental study. Cronemberger[6], *et al.* investigated the interior ballistics of 7.62 mm barrel by Vallier-Heydenreich method, lumped parameter method, PRODAS simulation and also experimentally. When they compared obtained results with experimental results, they concluded that lumped parameter method and PRODAS simulation predict the best results for the maximum pressure. Chen & Liu[18] inversely estimate the time dependent heat flux and barrel inside temperature of 7.62mm barrel in their numerical model. Chung[19], *et al.* found heat input by measured bore temperature values, then they presented an empirical equation for the wear rate of a 40 mm barrel as a function of heat input for two different types of ammunition. Mishra[20], *et al.* used exponentially decaying heat flux in their numerical model for 155 mm, 52 caliber barrel and validated their model with experimental results. Hill and Conner[21] proposed a one-dimensional numerical model which yields temperature distribution through the thickness of the barrel. In their model thermal conductivity and specific heat of the barrel are temperature dependent and they obtained gas temperature by PRODAS for the interior wall boundary condition. Yong-hai[22] presented temperature distribution on the barrel under the effects of thermal and pressure pulses by his numerical model which considers temperature dependent physical properties of the barrel. Akçay & Yükselen[23] applied his one-dimensional numerical model to 7.62 mm M60 machine gun for serial shots. They obtained thermodynamic characteristics of combustion gases and heat convection coefficient inside the barrel by means of interior ballistics code. This model considers specific heat and thermal conductivity of the barrel as temperature dependent. Shen[24], *et al.* developed time dependent thermo-mechanical finite element model for the simulation of the interior ballistics process of the bullet-barrel system. They concluded that main factors responsible for the life end of 12.7 mm barrel are the variation of the bullet's surface morphology and the increase of its disturbance at the muzzle. Li[25], *et al.* established the relationship between chromium coating surface temperature and interface shear damage by finite element method and in-situ tensile test in their study. They concluded that increasing the crack spacing of chromium coating and also coating thickness will extend the service life of the gun barrel.

In this study, thermal behaviour a 120 mm smoothbore cannon barrel has been investigated numerically by COMSOL Multiphysics finite element modelling and simulation software. It is aimed to present temperature distribution inside a cannon barrel by using a proposed heat transfer model based on the determination of the inner surface heat transfer coefficient, which varies with time during the interior ballistics, being influenced by projectile velocity, dynamic viscosity, thermal conductivity, density and Prandtl number of the propellant burned gas. Thermophysical properties of combustion gas have been obtained considering the combustion equation of the propellant and the PRODAS interior ballistics simulation. This study presents very detailed analysis for the heat transfer inside the cannon barrel and a new procedure to evaluate the heat transfer coefficient on inner barrel surface. Furthermore, a new approach is provided combining the PRODAS simulation of the interior ballistics with the COMSOL simulation of the heat transfer in the barrel.

## 2. MATERIAL AND METHODS

### 2.1 Geometry and Theoretical Model

In this study, interior ballistics and temperature distribution of the cannon barrel has been investigated by proposed numerical model. Geometry of the investigated cannon barrel is presented in Fig. 1.

Geometric dimensions of the investigated cannon barrel with the length of 4.826m are presented also in Table 1.

The numerical model has been presented by Eqns (1-9). Analysis has been performed in axisymmetric two-dimensional geometry.

$$\frac{1}{r}\frac{\partial}{\partial r}\left(k_{steel} r \frac{\partial T}{\partial r}\right)+\frac{\partial}{\partial z}\left(k_{steel}\frac{\partial T}{\partial z}\right)=\rho_{steel}c_{steel}\frac{\partial T}{\partial t} \quad (1)$$

$$h_S\left(T_S-T_{in}\right)=-k_{steel}\left.\frac{\partial T}{\partial r}\right|_{r=R_{in}} \quad (2)$$

$$h_{out}\left(T_{out}-T_{air}\right)+\varepsilon\sigma\left(T_{out}^{\ 4}-T_{air}^{\ 4}\right)=-k_{steel}\left.\frac{\partial T}{\partial r}\right|_{r=R_{out}} \quad (3)$$

$$\left.\frac{\partial T}{\partial z}\right|_{z=0}=0 \quad (4)$$

$$\left.\frac{\partial T}{\partial z}\right|_{z=L}=0 \quad (5)$$

$$T\big|_{t=0}=T_0=20^o C \quad (6)$$

$$T_{air}=20^o C \quad (7)$$

$$T_S=\begin{cases}T_{gas} & z<S(t)\\ T_0 & z\geq S(t)\end{cases} \quad (8)$$

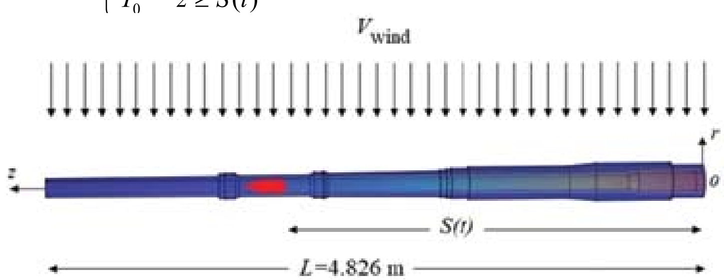


**Figure 1. Geometry of the cannon barrel.**

$$h_S=\begin{cases}h_{in} & z<S(t)\\ 0 & z\geq S(t)\end{cases} \quad \text{for single shot} \quad (9)$$

where $T_S$ is temperature of the inside medium of the barrel, $T_{in}$ is temperature at the inner surface of the barrel, $\varepsilon$ is the emissivity of the barrel surface having the value of 0.85 [13] and $\sigma$ is Stefan-Boltzmann constant ($5.67\cdot10^{-8}$W/m$^2$K$^4$). Similar to the function of $T_S$, convection heat transfer coefficient inside the barrel, $h_S$, is calculated as a function of projectile position $S$ considering internal convection heat transfer coefficient before the projectile, $h_{in}$.

Thermophysical properties of the cannon barrel are taken from the study of Gerber and Bundy[27] and given in Table 2. Temperature dependent functions of specific heat and thermal conductivity of the steel have been obtained by curve fitting. Temperature in these functions are in Kelvin ($K$). $R^2$ is the coefficient of determination. It ranges from 0 to 1. Values of $R^2$ closer to 1 shows the fitted curve is better.

Figure 2 shows projectile position, velocity of the projectile, temperature inside the gun and breech pressure during interior ballistics, which have been obtained by PRODAS for the ammunition of 120 mm M829 APFSDS-T with the propellant of JA-2[28]. PRODAS is a commercial interior ballistics software with a data library of guns and ammunitions, having also different solvers. So, the results have been obtained in the PRODAS for the Baer and Frankle interior ballistics model, 120 mm gun and M829 APFSDS-T ammunition.

It is important to highlight that the model, adopted in the PRODAS simulation, considers a shot start pressure of 1.4445 MPa. Then, following this approach, the interior ballistics starts when the pressure in the combustion chamber reaches the start pressure. The time before such instant is neglected, since until this time, the burned hot gases are not in touch with the barrel. So, in this simulation, the interior ballistics starts with the movement of the projectile.

The key point to model the heat transfer inside the barrel structure is to obtain heat convection coefficient on the inner surface of the barrel. Detailed thermophysical

**Table 1. Geometric dimensions of the cannon barrel[26]**

| Distance from breech $z$ (m) | Corresponding inner radius $R_{in}$ (mm) | Distance from breech $z$ (m) | Corresponding outer radius $R_{out}$ (mm) | Distance from breech $z$ (m) | Corresponding outer radius $R_{out}$ (mm) |
|---|---|---|---|---|---|
| 0 | 79.55 | 0 | 135 | 2.762 | 98 |
| 0.061 | 78.8 | 0.237 | 135 | 2.788 | 112.5 |
| 0.486 | 78.8 | 0.238 | 154.95 | 2.804 | 112.5 |
| 0.555 | 60.4 | 0.8 | 154.95 | 2.805 | 108 |
| 0.805 | 60.05 | 1 | 135 | 2.868 | 108 |
| 4.826 | 60.05 | 1.731 | 135 | 2.898 | 89 |
| | | 1.732 | 125 | 3.415 | 89 |
| | | 1.863 | 125 | 3.445 | 108 |
| | | 1.864 | 120 | 3.520 | 108 |
| | | 1.9 | 120 | 3.521 | 105 |
| | | 1.901 | 112.5 | 3.560 | 105 |
| | | 1.940 | 112.5 | 3.561 | 85.5 |
| | | 1.950 | 107.5 | 4.826 | 80.5 |

**Table 2. Thermophysical properties of the barrel**

| | | | |
|---|---|---|---|
| $c_{steel}$ **(J/kgK)** | $417.1728 + 5.32 \cdot 10^{-2}T + 3 \cdot 10^{-4}T^2$ | $3.03\text{K} \leq T \leq 969.7\text{K}$ | $R^2 = 0.9955$ |
| | $-15849.8609 + 17.1011T$ | $969.7\text{K} \leq T \leq 1016.67\text{K}$ | $R^2 = 0.9862$ |
| | $11850.4603 - 10.1614T$ | $1016.67\text{K} \leq T \leq 1119.7\text{K}$ | $R^2 = 0.9643$ |
| | $450.2656 + 0.1227T$ | $1119.7\text{K} \leq T$ | $R^2 = 0.9941$ |
| $k_{steel}$ **(W/mK)** | $5.9834 + 34.9813(1-e^{-0.00687})$ | $31.76\text{K} \leq T \leq 440.08\text{K}$ | $R^2 = 0.9990$ |
| | $36.4593 + 1.63 \cdot 10^{-2}T - 2.4696 \cdot 10^{-5}T^2$ | $440.08\text{K} \leq T \leq 1058.22\text{K}$ | $R^2 = 0.9996$ |
| | $14.1706 + 1.13 \cdot 10^{-2}T$ | $1058.22\text{K} \leq T$ | $R^2 = 0.9993$ |
| $\rho_{steel}$ **(kg/m³)** | 7827 | | |

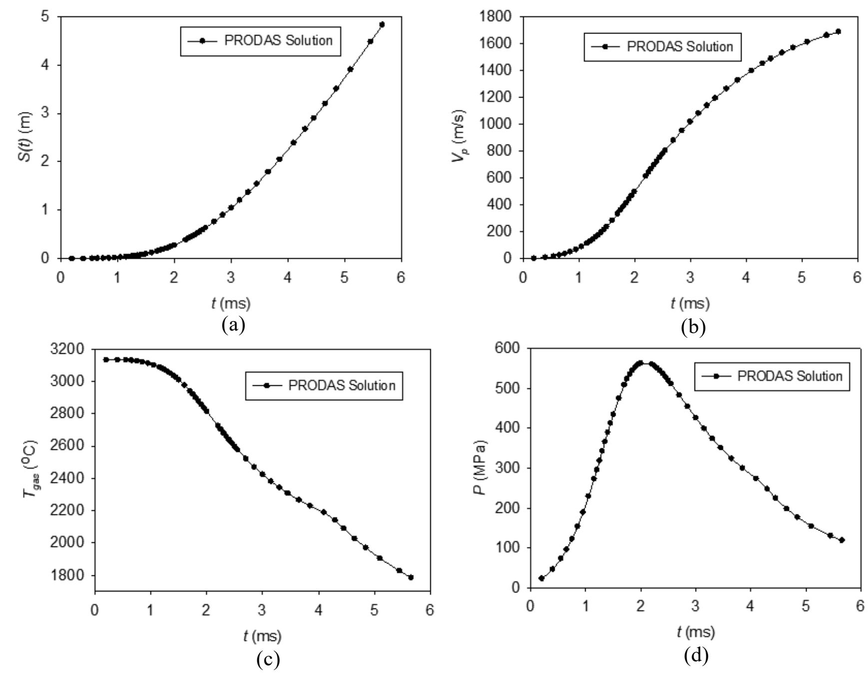


**Figure 2. PRODAS results: (a) Projectile position as a function of time, (b)Velocity of the projectile as a function of time, (c) Temperature of gas mixture inside the gun, and (d) Breech pressure inside the gun.**

analysis from the time of the propellant ignition until the end of the interior ballistics is needed for the calculation of the heat convection coefficient inside the gun.

## 2.2 Calculation of the Heat Convection Coefficients Inside and Outside the Barrel

Products of the combustion equation and their dependent thermophysical properties need to be known for the calculation of inside convection coefficient $h_{in}$. Chemical composition of the JA-2 has been presented in Table 3.

A general combustion equation for the propellant is present in Eqn (10)[31] and the combustion equations for each propellant ingredient are presented in Eqns (11-16).

$$C_aH_bN_cO_dCl_eS_f \rightarrow aCO_2 + \frac{1}{2}(b-e)H_2O + \frac{c}{2}N_2 + eHCl + fSO_2 - \left\{(a+f) + \frac{1}{4}(b-e) - \frac{d}{4}\right\}O_2 \quad (10)$$

$$C_{12}H_{14}N_6O_{22} \rightarrow 12\ CO_2 + 7\ H_2O + 3\ N_2 - 4.5\ O_2 \quad (11)$$

**Table 3. JA-2 Propellant formulation[29,30]**

| Ingredients | Chemical formula | Molecular weight (g/mol) | Weight % |
|---|---|---|---|
| Nitrocellulose (13.4 % N) (NC) | $C_{12}H_{14}N_6O_{22}$ | 594.2696 | 59.5 |
| Nitroglycerin (NG) | $C_3H_5N_3O_9$ | 227.0872 | 14.9 |
| Diethylene glycol dinitrate (DEGDN) | $C_4H_8N_2O_7$ | 196.1164 | 24.8 |
| Ethyl centralite | $C_{17}H_{20}N_2O$ | 268.3578 | 0.7 |
| Magnesium oxide | MgO | 40.3044 | 0.05 |
| Graphite | C | 12.011 | 0.05 |

$$C_3H_5N_3O_9 \rightarrow 3\ CO_2 + 2.5\ H_2O + 1.5\ N_2 + 0.25\ O_2 \quad (12)$$

$$C_4H_8N_2O_7 \rightarrow 4\ CO_2 + 4\ H_2O + N_2 - 2.5\ O_2 \quad (13)$$

$$C_{17}H_{20}N_2O \rightarrow 17\ CO_2 + 10\ H_2O + N_2 - 21.5\ O_2 \quad (14)$$

$$MgO \rightarrow Mg + 0.5\ O_2 \quad (15)$$

$$C \rightarrow CO_2 - O_2 \quad (16)$$

It has been known that the JA-2 propellant is consisting of $a_1$, $b_1$, $c_1$, $d_1$, $e_1$ and $f_1$ moles of $C_{12}H_{14}N_6O_{22}$, $C_3H_5N_3O_9$, $C_4H_8N_2O_7$, $C_{17}H_{20}N_2O$, MgO and C, respectively as shown in Eqn (17). These constants can easily be found as a function of proportionality constant $n$ by using weight percentages of each ingredient of JA-2 and their molecular weights.

$$JA-2 \rightarrow a_1C_{12}H_{14}N_6O_{22} + b_1C_3H_5N_3O_9 + c_1C_4H_8N_2O_7 + d_1C_{17}H_{20}N_2O + e_1MgO + f_1C \quad (17)$$

$$a_1 = 0.100122907n \quad (18)$$

$$b_1 = 0.065613561n \quad (19)$$

$$c_1 = 0.126455513n \quad (20)$$

$$d_1 = 0.002608458n \quad (21)$$

$$e_1 = 0.001240559n \quad (22)$$

$$f_1 = 0.004162851n \quad (23)$$

It can be easily seen that the effects of the ethyl centralite ($C_{17}H_{20}N_2O$), magnesium oxide (MgO) and graphite (C) can be neglected in the combustion equation. Eqn (24) can easily be obtained when selecting $a_1$ = 100, $b_1$ = 66 and $c_1$ = 126 in the case of complete burning. But in the real case, there should be $H_2$ and CO in the combustion products due to incomplete burning because of the insufficient oxygen in the medium. The combustion equation in the case of incomplete burning has been obtained and presented in Eqn (25) to be used for calculations. Real combustion equation of propellant JA-2 can easily be obtained after assuming mole fraction of $CO_2$ to that of CO in the products as 1.5, following Değirmenci and Dirikolu[32].

Combustion equation of JA-2 in the case of complete burning:

$$100\ C_{12}H_{14}N_6O_{22} + 66\ C_3H_5N_3O_9 + 126\ C_4H_8N_2O_7 + 748.5\ O_2 \rightarrow 1902\ CO_2 + 1369\ H_2O + 525\ N_2 \quad (24)$$

Combustion equation of JA-2 inside the barrel:

$$100\ C_{12}H_{14}N_6O_{22} + 66\ C_3H_5N_3O_9 + 126\ C_4H_8N_2O_7 \rightarrow 1141.2\ CO_2 + 760.8\ CO + 632.8\ H_2O + 525\ N_2 + 736.2\ H_2 \quad (25)$$

Thermophysical properties of each combustion gases depending on temperature has been calculated by using data in the NIST[33] website and curve fitting method. Temperature dependent functions of thermophysical properties are presented in Table 4. In these correlations temperature is in Celsius (°C).

Volume behind the projectile during the movement of the projectile and mass fraction have been obtained by PRODAS. Time dependent variations of the volume behind the projectile, mass fraction, mass and density of the combustion gases are presented in Figs. 3 and 4. As it can be seen from Figs. 3 and 4, volume behind the projectile shows exponential growth after 2 ms due to the motion of projectile position (Fig. 2(a)) and mass fraction increases almost linearly from 0 to 1 during the interior ballistic. Because at the beginning of the interior ballistics, propellant, which is in the combustion chamber, is in the solid form and there is no gas formation. During combustion of the solid propellant, mass of the combustion gases increases with the decrease of the solid propellant mass, as a result, mass fraction gets the value of 1 towards the end of the interior ballistics. Total mass and the density of the combustion gases have been obtained by the Eqns (26) and (27), respectively. Mass of propellant is 7.9 kg. Mass fraction of the combustion gases increases almost linearly until the propellant is consumed. While density of the combustion gases also increases almost linearly until 2 ms, it decreases after this time due to the exponential growth of the volume behind the projectile.

**Table 4. Thermophysical properties of combustion gases**

| | | |
|---|---|---|
| **Dynamic viscosity (Pas)** | $\mu_{CO_2} = 8.6759\cdot10^{-5} + 2\cdot10^{-4}e^{(-3.9\cdot10^{-3}T)}$ | $R^2$=1 |
| | $\mu_{CO} = 4.0845\cdot10^{-5} + 1.9629\cdot10^{-5}e^{(-1.1\cdot10^{-2}T)}$ | $R^2$=1 |
| | $\mu_{H_2O} = 6.8442\cdot10^{-5} + 3\cdot10^{-4}e^{(-3.9\cdot10^{-3}T)}$ | $R^2$=0.9996 |
| | $\mu_{N_2} = 7.5009\cdot10^{-5} - 1.5899\cdot10^{-8}T + 1.0079\cdot10^{-11}T^2$ | $R^2$=0.9915 |
| | $\mu_{H_2} = 2.2575\cdot10^{-5} - 4.4447\cdot10^{-9}T + 9.5023\cdot10^{-12}T^2$ | $R^2$=0.9997 |
| **Thermal conductivity (W/mK)** | $k_{CO_2} = 0.1559 - 1.6511\cdot10^{-5}T$ | $R^2$=0.9331 |
| | $k_{CO} = 0.1043 + 0.2636e^{(-5.9\cdot10^{-3}T)}$ | $R^2$=1 |
| | $k_{H_2O} = 0.1510 + 3.1215e^{(-3.5\cdot10^{-3}T)}$ | $R^2$=0.9999 |
| | $k_{N_2} = 0.1313 - 2.0240\cdot10^{-5}T + 1.529\cdot10^{-8}T^2$ | $R^2$=0.9952 |
| | $k_{H_2} = 0.7893 + 7\cdot10^{-4}T - 5.1201\cdot10^{-8}T^2$ | $R^2$=1 |
| **Prandtl number** | $Pr_{CO_2} = 0.8193 + 0.8391e^{(-2.4\cdot10^{-3}T)}$ | $R^2$=1 |
| | $Pr_{CO} = 0.2204 + 2\cdot10^{-4}T + 7.7388\cdot10^{-7}T^2$ | $R^2$=1 |
| | $Pr_{H_2O} = -0.1318 + 1.6\cdot10^{-3}T - 3.7592\cdot10^{-7}T^2$ | $R^2$=0.9998 |
| | $Pr_{N_2} = 0.6796 + 2.1064\cdot10^{-5}T + 5.7657\cdot10^{-10}T^2$ | $R^2$=0.9963 |
| | $Pr_{H_2} = 0.2895 + 0.3821e^{(-6.6\cdot10^{-3}T)}$ | $R^2$=0.9998 |

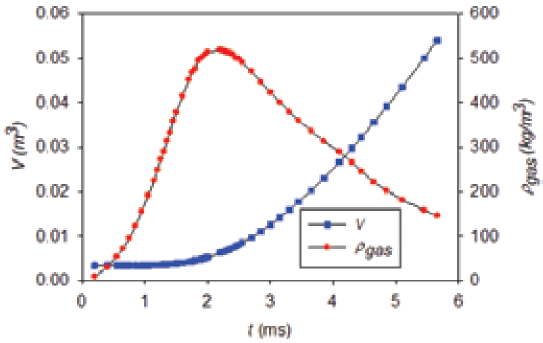


**Figure 3. Volume behind the projectile and density of gas mixture.**

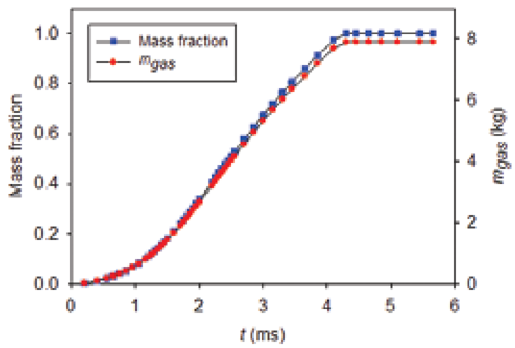


**Figure 4. Mass fraction and mass of the gas mixture.**

$$mass\ \ fraction(t) = \frac{m_{gas}(t)}{m_{propellant}} \tag{26}$$

$$\rho_{gas}(t) = \frac{m_{gas}(t)}{V(t)} \tag{27}$$

Dynamic viscosity, thermal conductivity and the Prandtl number (*Pr*) of the burned gas mixture have been calculated considering Eqn (25), as in the study of Değirmenci and Dirikolu[32], and presented by Eqns (28)-(30), respectively. These thermophysical properties of the gas mixture have been obtained using temperature dependent functions for each gas presented in Table 4 and the gas mixture temperature inside the barrel shown in Fig. 2(c). The obtained results are presented in Figs. 5 and 6.

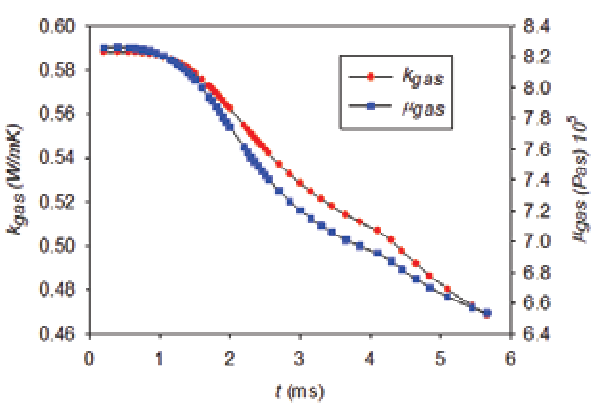


**Figure 5. Thermal conductivity and dynamic viscosity of the gas mixture.**

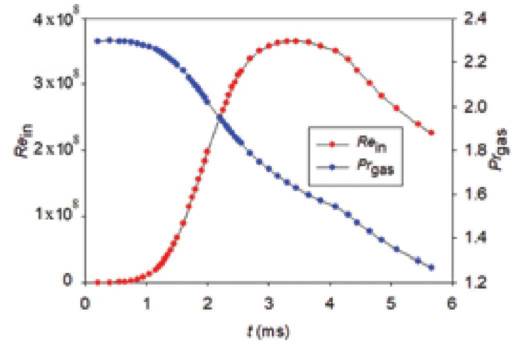


**Figure 6. Reynolds number ($Re_{in}$) and Prandtl number ($Pr_{gas}$) of the gas mixture.**

$$\mu_{gas} = \frac{1141.2\mu_{CO_2} + 760.8\mu_{CO} + 632.8\mu_{H_2O} + 525\mu_{N_2} + 736.2\mu_{H_2}}{3796} \tag{28}$$

$$k_{gas} = \frac{1141.2k_{CO_2} + 760.8k_{CO} + 632.8k_{H_2O} + 525k_{N_2} + 736.2k_{H_2}}{3796} \tag{29}$$

$$\Pr_{gas} = \frac{1141.2\Pr_{CO_2} + 760.8\Pr_{CO} + 632.8\Pr_{H_2O} + 525\Pr_{N_2} + 736.2\Pr_{H_2}}{3796} \tag{30}$$

Dittus–Boelter equation[32,34] has been used for the calculation of the time dependent internal convection heat transfer coefficient of the 120mm caliber gun barrel. Half of the projectile velocity has been used for the calculation of the Reynolds number ($Re_{in}$), representing the characteristic velocity of the burned gas mixture. Time dependent variation of the Reynolds number inside the barrel has also been presented in Fig. 6. This hypothesis is based on the fact that the gases at the breech are stationary and the velocity of the projectile is equal to the gas velocity behind the projectile. So, there is a gas velocity gradient from the breech to the projectile. Heat convection coefficient inside the barrel during the interior ballistics has been presented in Fig. 7.

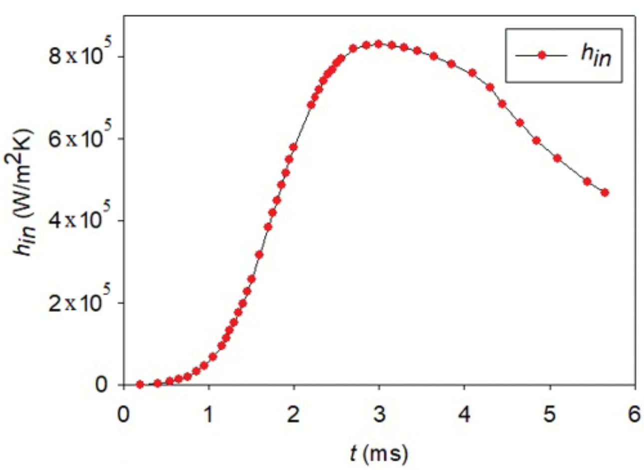


**Figure 7. Convection heat transfer coefficient inside the barrel during interior ballistics.**

$$Nu_{in}(t) = \frac{h_{in}(t)D_{in}}{k_{gas}(t)} = 0.023\,\mathrm{Re}_{in}(t)^{0.8}\,\mathrm{Pr}_{gas}(t)^{0.3} \tag{31}$$

$$\mathrm{Re}_{in}(t) = \frac{0.5V_p(t)D_{in}\rho_{gas}(t)}{\mu_{gas}(t)} \tag{32}$$

It is noteworthy that the convective heat transfer coefficient inside the barrel considers the data provided by PRODAS and Baer and Frankle model assumptions, including the single-phase burned gas flow inside the gun.

Convection coefficient outside of the barrel has been found as 13.4W/m²K by the correlation given in Eqn (33)[13,34]. Outside air velocity was assumed as 10km/h. Thermophysical properties of the air was evaluated at the film temperature, which is the mean of medium air and outside barrel temperatures. So, discrepancy analysis of the convection coefficient outside of the barrel has been performed considering outside barrel temperature values from 20 °C to 140 °C. Maximum discrepancy for $h_{out}$ has been calculated as 2.4% and it has been concluded that variation of the outside convection coefficient of the barrel due to the outside barrel surface temperature can be neglected.

$$Nu_{out} = \frac{h_{out}D_{out}}{k_{air}} = 0.3 + \frac{0.62\,\mathrm{Re}_{out}^{1/2}\,\mathrm{Pr}_{air}^{1/3}}{\left[1+\left(0.4/\mathrm{Pr}_{air}\right)^{2/3}\right]^{1/4}}\left[1+\left(\frac{\mathrm{Re}_{out}}{282000}\right)^{5/8}\right]^{4/5}$$

$$\mathrm{Re}_{out}\,\mathrm{Pr}_{air} > 0.2 \tag{33}$$

## 3. RESULTS AND DISCUSSION

Mesh dependency analysis has been performed for the study as shown on Fig. 8. It has been observed that no significant change on the results was observed with 4626496 and more elements. As a result, analysis have been performed with 4626496 triangular elements in this study. $T_{ave\_in}$ is the average temperature at the inner surface of the barrel. Maximum and average growth rates for the mesh used in this study are respectively 2.205 and 1.008. Minimum and average element quality values are also 0.6756 and 0.9922, respectively.

Barrel section from z = 0.3 m to z = 0.9 m from the breech was considered for the validation as shown in Fig. 9a. Validation of the code has been performed considering temperature variation at the cross section of the barrel at z = 0.6m from breech as shown in Fig. 9(b). As temperature variation in a very thin layer from the inside surface of the barrel has been considered, 12463872 elements was used for the barrel geometry with 0.11 mm chromium layer on its inside surface and 1463872 elements was used for the barrel geometry without chromium layer. Time dependent gas temperature and convection coefficient given for the cross section at z=0.6m from the study of Underwood[35], *et al.* have been applied on inner surface of the barrel for the validation of the code used in this study. Although both numerical results show good agreement with the literature, chromium coating ones are generally closer to Underwood[35], *et al.* results as expected.

Simulations of temperature and projectile position inside the gun were obtained and given in Fig. 10. Combustion starts at the combustion chamber and hot gases moves along the barrel from combustion chamber to the muzzle. As a result, the hottest place is the combustion chamber inside the gun. As it can be seen from Figs. 10(a) and 11, the highest value of the inside barrel temperature is observed at 3 ms due to the behaviour of the convection heat transfer coefficient inside the barrel (Fig. 7). Although gas temperature inside the gun decreases with time as seen from Fig. 2(c), the convection heat transfer coefficient of combustion gases increases until 3ms and then decreases. It has been concluded that convective

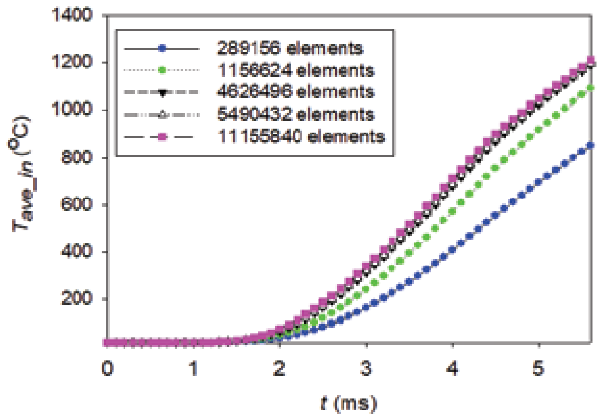


**Figure 8. Effects of the number of mesh elements on average temperature at the inner surface of the barrel.**

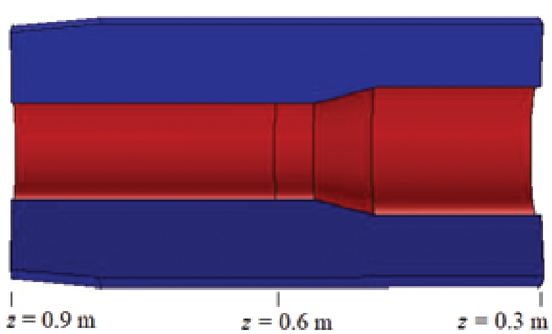


(a)

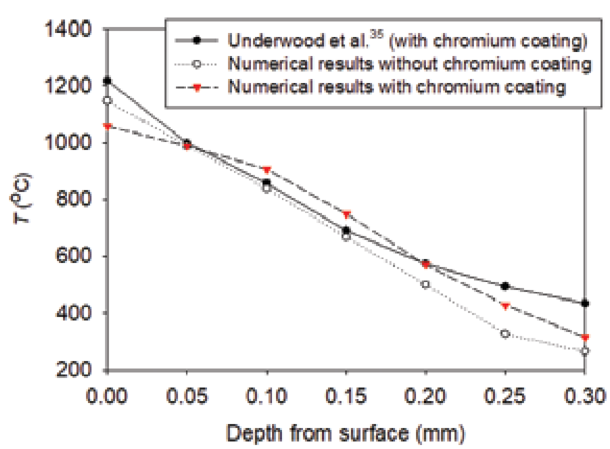


(b)

**Figure 9. Geometry of the barrel and validation of the code: (a) Barrel geometry and (b) Temperature variation at the cross section of the barrel at z = 0.6 m from the breech (t = 4 ms).**

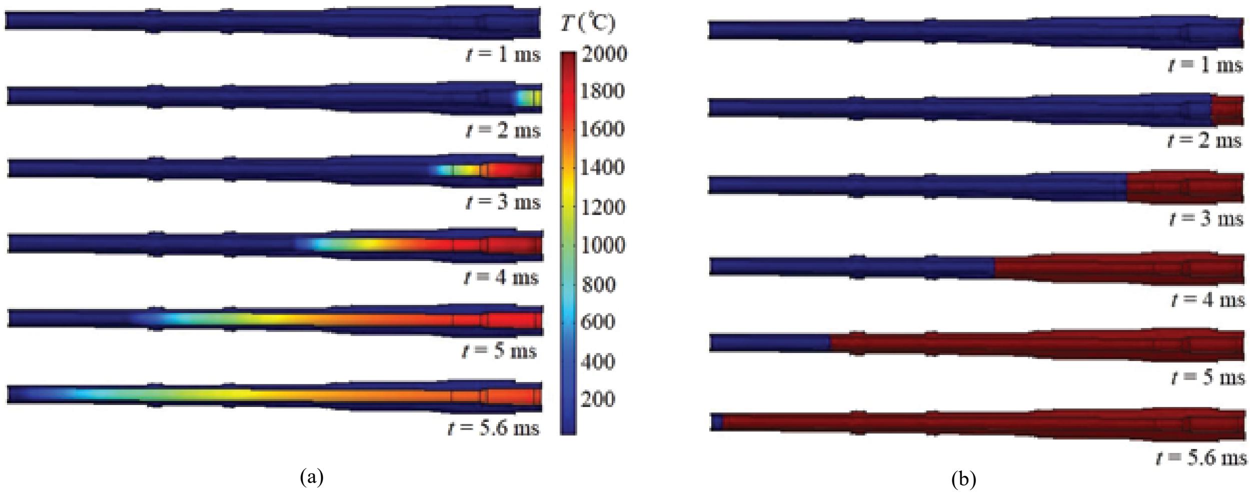


**Figure 10. Simulations inside the cannon barrel during interior ballistics: (a) Temperature and (b) Projectile position.**

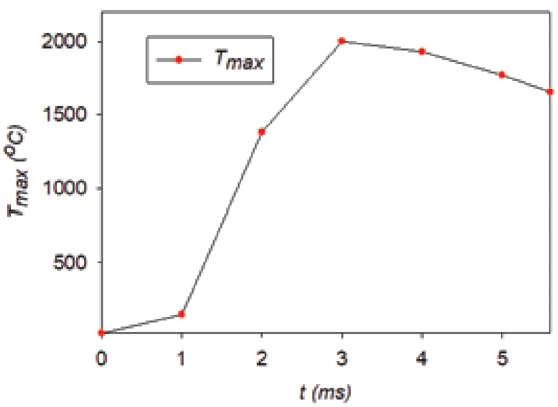


**Figure 11. Maximum temperature value inside the barrel.**

heat transfer coefficient of combustion gases has an important effect on the heat transfer inside the barrel. On the other hand, maximum value of the temperature inside the barrel decreases after 3ms by the effects of the projectile motion and decrease of the convection heat transfer coefficient inside the barrel. Rather than conduction, heat transfer by convection due to the movement of the projectile has an important role on the transformation of heat to other parts of the barrel during interior ballistics.

The red coloured places in Fig. 10(b) are places occupied by hot combustion gases. The intersection of the blue and red coloured places also shows the position of the projectile. As it can be seen from Fig. 2(a) and simulations in Fig. 10(b), projectile motion inside the barrel shows exponential growth. The total interior ballistics time is 5.659 ms. It is also shown from Fig. 10(b) that projectile is about to leave the muzzle at 5.6 ms.

## 4. CONCLUSION

In this paper a new and detailed numerical model has been proposed for the prediction of the thermal behaviour of a cannon barrel during interior ballistics. This new approach combines PRODAS interior ballistics simulation with COMSOL simulation of the heat transfer inside the barrel. The new procedure to compute the convective heat transfer coefficient on the inner barrel surface considers the interior ballistics data, chemical propellant combustion equation and temperature dependent thermophysical properties of the burned gas mixture.

The simulations were performed considering the 120mm gun with a M829 APFSDS-T ammunition and results reveals the temperature evolution inside the barrel structure along of the time. Moreover, the maximum temperature in the barrel and the convection heat transfer coefficient inside the barrel reach those maximum values almost at the same instant at 3ms after fire. So, it is possible to conclude that there is a strong influence of the convection coefficient inside the barrel on the maximum temperature of the barrel. Consequently, it was verified that the convection coefficient on the inner barrel surface is really a key function to be modelled. Furthermore, the convective heat transfer coefficient of burned gases inside the gun has major effect than the burned gas temperature on the heat transfer phenomenon, since the maximum combustion gas temperature occurs at 0.4 ms after fire.

The proposed approach is feasible and useful to model and simulate the heat transfer in a barrel and to compute the convective heat transfer coefficient inside the gun, which is relevant to investigate many interior ballistics problems influenced by the temperature as wear, cook-off and thermal stress in the barrel.

## REFERENCES

1. Carlucci, D.E. & Jacobson, S.S. Ballistics: theory and design of guns and ammunition, CRC Press, Boca Raton, USA, 2008.
2. Koç, M.A.; Esen, İ. & Çay, Y. Tip deflection determination of a barrel for the effect of an accelerating projectile before firing using finite element and artificial neural network combined algorithm. *Lat. Am. J. Solids Struct.*, 2016, **13**(10), 1968–1995. doi: 10.1590/1679-78252718.
3. Esen, I & Koç, M.A. Dynamic response of a 120 mm smoothbore tank barrel during horizontal and inclined firing positions. *Lat. Am. J. Solids Struct.*, 2015, **12**(8), 1462–1486.

doi: 10.1590/1679-78251576.
4. Koç, M.A.; Esen; İ. & Çay, Y. Dynamic analysis of gun barrel vibrations due to effect of an unbalanced projectile considering 2-D transverse displacements of barrel tip using a 3-D element technique. *Lat. Am. J. Solids Struct*., 2018, **15**(9), 1-21.
doi: 10.1590/1679-78254972.
5. Esen, I & Koç, M.A. Optimization of a passive vibration absorber for a barrel using the genetic algorithm. *Expert Syst. Appl.*, 2015, **42**(2), 894-905.
doi: 10.1016/j.eswa.2014.08.038.
6. Cronemberger, P.O.; Júnior, E.P.L.; Gois, J.A.M. & Caldeira, A.B. Theoretical and experimental study of the interior ballistics of a rifle 7.62, *Engenharia Térmica (Therm. Engineering)*, 2014, **13**(2), 20-27.
doi: 10.5380/reterm.v13i2.62089.
7. Boisson, D.; Légeret, G. & Barthélémy, J.F. Experimental investigation of heat transfer in a 120 mm testing gun barrel based on a space marching finite difference algorithm for the inverse conduction method. *In* 19th International Symposium of Ballistics: Interlaken, Switzerland, 2001, pp. 163-170.
8. Franco, P. & Peter, H. Gun Barrel Erosion: Study of thermally insulating layers. *In* 19th International Symposium of Ballistics: Interlaken, Switzerland, 2001, pp. 315-321.
9. Wildegger-Gaissmaier, A.E. Barrel heating simulation for 5″/54 guns using the XBR-2D code. Defence Science and Technology Organization, Department of Defence, Aeronautical and Maritime Research Laboratory, Australia, Report No. DSTO-TR-0098, 1994.
10. Chen, T.C.; Liu, C.C.; Jang, H.Y. & Tuan, P.C. Inverse estimation of heat flux and temperature in multi-layer gun barrel. *Int. J. Heat Mass Transf.*, 2007, **50**(11-12), 2060-2068.
doi: 10.1016/j.ijheatmasstransfer.2006.11.022.
11. Mishra, A.; Hameed, A. & Lawton, B. Assessment of variable thermophysical properties on temperature history of a 155 mm gun barrel using ANSYS. *In* International Conference on Methods and Models in Computer Science: Delhi, India, 2009.
doi: 10.1109/ICM2CS.2009.5397974.
12. Şentürk, A.; Işık, H. & Evci, C. Thermo-mechanically coupled thermal and stress analysis of interior ballistics problem. *Int. J. Therm. Sci.*, 2016, **104**, 39-53.
doi: 10.1016/j.ijthermalsci.2015.12.019.
13. Işık, H. & Göktaş, F. Cook-off analysis of a propellant in a 7.62 mm barrel by experimental and numerical methods. *Appl. Therm. Eng.*, 2017, **112**, 484-496.
doi: 10.1016/j.applthermaleng.2016.10.104.
14. Copley, J.A. & Thomas, W.C. Two-dimensional transient temperature distribution in cylindrical bodies with pulsating time and space-dependent boundary conditions. *J. Heat Transf.*, 1974, **96**(3), 300-306.
doi: 10.1115/1.3450196.
15. Hansen, E.C. & Heiney, O.K. Pressure and gas flow gradients behind the projectile during the interior ballistic cycle. *In*: 10th International Symposium on Ballistics: San Diego, California, A.B.D., 1987.
16. Bundy, M.L.; Conroy, P.J. & Kennedy, J.L. Simulated and experimental in-wall temperatures for 120 mm ammunition. *Def. Sci. J.,* 1996, **46**(4), 223-232.
doi: 10.14429/dsj.46.4081.
17. Hameed A.; Azavedo, M. & Pitcher, P. Experimental investigation of a cook-off temperature in a hot barrel. *Def. Technol.*, 2014, **10**(2) 86-91.
doi: 10.1016/j.dt.2014.05.006.
18. Chen, T.C. & Liu, C.C. Inverse estimation of time-varied heat flux and temperature on 2-D gun barrel using input estimation method with finite-element scheme. *Def. Sci. J.*, 2008, **58**(1), 57-76.
doi: 10.14429/dsj.58.1623.
19. Chung, D.Y.; Shin, N.; Oh, M.; Yoo, S.H. & Nam, S.H. Prediction of erosion from heat transfer measurements of 40 mm gun tubes. *Wear*, 2007, **263**(1-6), 246-250.
doi: 10.1016/j.wear.2006.12.065.
20. Mishra, A.; Hameed, A. & Lawton, B. A novel scheme for computing gun barrel temperature history and its experimental validation. *J. Press. Vessel Technol.*, 2010, **132**(6), 061202.
doi: 10.1115/1.4001740.
21. Hill, R.D. & Conner, J.M. Transient heat transfer model of machine gun barrels. *Mater. Manufacturing Processes*, 2012, **27,** 840-845.
doi: 10.1080/10426914.2011.648694.
22. Yong-hai, W. Analysis of the temperature field of a gun tube based on thermal-solid coupling. *Res. J. Appl. Sci., Eng. Technol.*, 2013, **5**(16) 4110-4117.
doi: 10.19026/rjaset.5.4634.
23. Akçay, M. & Yükselen, M.A. Unsteady thermal studies of gun barrels during the interior ballistic cycle with non-homogenous gun barrel material thermal characteristics. *J. Therm. Sci. Technol. (Isı Bilimi ve Tekniği Derg.)*, 2014, **34**(2), 75-81.
24. Shen, C.; Zhou, K.; Lu Y. & Li J., Modeling and simulation of bullet-barrel interaction process for the damaged gun barrel. *Def. Technol.*, 2019, **15**(6), 972-986.
doi: 10.1016/j.dt.2019.07.009.
25. Li, X.; Zang, Y.; Lian, Y.; Ma, M.; Mu, L. & Qin, Q. An interface shear damage model of chromium coating/steel substrate under thermal erosion load. *Def. Technol.*, 2021, **17**(2), 405-415.
doi: 10.1016/j.dt.2020.02.002.
26. Gerber, N. & Bundy M.L. Heating of a tank gun barrel: numerical study. Ballistic Research Laboratory Aberdeen Proving Ground, Maryland, USA, Memorandum Report Brl-Mr-3932, 1991.
27. Gerber, N. & Bundy M.L. Effect of variable thermal properties on gun tube heating. Ballistic Research Laboratory Aberdeen Proving Ground, Maryland, USA, Memorandum Report Brl-Mr-3984, 1992.
28. Military, M829 120mm, APFSDS-T. https://www.globalsecurity.org/military/systems/munitions//m829a1.htm , (accessed 3 October 2020).
29. Reese, D.A.; Groven, L.J. & Son, S.F. Formulation and characterization of a new nitroglycerin-free double base

propellant. *Propellants, Explosives, Pyrotechnics*, 2014, **39**(2), 205-210.
doi: 10.1002/prep.201300105.

30. Conner C.B. & Anderson, W.R. Modeling the combustion of JA2 and solid propellants of similar composition. *Proc. Combustion Inst.*, 2009, **32**(2), 2131-2137.
doi: 10.1016/j.proci.2008.06.059.
31. Kubota N., Propellant and explosives: thermochemical aspects of combustion. Wiley-VCH, Germany, 2002.
32. Değirmenci, E. & Drikolu, M.H. A thermochemical approach for the determination of convection heat transfer coefficients in a gun barrel. *Appl. Therm. Eng.*, 2012, **37**, 275-279.
doi: 10.1016/j.applthermaleng.2011.11.029.
33. NIST Chemistry WebBook, SRD 69, thermophysical properties of fluid systems. https://webbook.nist.gov/chemistry/fluid/ , (Accessed 3 October 2020).
34. Çengel, Y.A. Heat transfer: a practical approach, second ed. McGraw-Hill, New York, 2003.
35. Underwood, J.H.; Witherell, M.D.; Sopok, S.; McNeil, J.C.; Mulligan, C.P. & Vigilante G.N. Thermomechanical modeling of transient thermal damage in cannon bore materials. *Wear*, 2004, **257**(9-10), 992-998.
doi: 10.1016/j.wear.2004.07.008.

## CONTRIBUTORS

**Dr Çiğdem Susantez** graduated from the Mechanical Engineering Department of Trakya University in 2007 and received her PhD in 2015 from the same University. She has been working as an Instructor Dr. at Mechanical Engineering Department of Trakya University. Her main research fields are interior ballistics, genetic algorithms, fluid mechanics, heat and mass transfer, nanofluids and phase change materials.
She had applied the presented numerical model to cannon barrel and performed numerical analysis.

**Dr Aldélio Bueno Caldeira** graduated, Cum Laude, from the Mechanical Engineering Department of Federal University of Rio de Janeiro (UFRJ) in 1995 and received his DSc in 2004 from UFRJ. He has been working in the Brazilian Army since 1997 and was Professor and Dean of Research, Extension and Innovation of Military Institute of Engineering. He is the Head of the Management and Technological Innovation Agency of the Brazilian Army (AGITEC). His main research fields are heat transfer, combustion, aerodynamics, optimisation and inverse problems.
He obtained variables of interior ballistics for cannon to be used in the numerical analysis. He had also conducted the modelling.